Quantitative Analysis of Lipid−Lipid and Lipid−Protein Interactions in Membranes by Use of Pyrene-Labeled Phosphoinositides†

E. H. W. Pap,‡ A. Hanicak,§ A. van Hoek,‡ K. W. A. Wirtz,|| and A. J. W. G. Visser*,‡

Department of Biochemistry, Agricultural University, Dreijenlaan 3, 6703 HA Wageningen, The Netherlands, Biophysics Institute, J.W. Goethe University, Theodor Stern Kai 7/H74, D-60590 Frankfurt am Main, Germany, and Centre for Biomembranes and Lipid Enzymology, Utrecht University, Padualaan 8, 3584 CH Utrecht, The Netherlands

Received July 29, 1994; Revised Manuscript Received April 17, 1995⊗

ABSTRACT: The lateral and rotational dynamics of phosphoinositides and their interactions with proteins were characterized using pyrene-labeled lipid analogues. In these systems, the collision frequency of pyrene-labeled lipids was studied by monitoring the monomeric pyrene fluorescence yield as a function of their mole fraction in the membranes. From this dependence, the lateral diffusion coefficient and a repulsion factor between two pyrene phosphoinositides could be estimated by applying an extended form of the Milling Crowd model [Eisinger, J., Flores, J., & Petersen, W. P. (1986) *Biophys. J. 49*, 987−1001]. The repulsion appeared to be highly dependent on the amount of negative charge of the lipid headgroups. From experiments with dioleoylphosphatidylcholine vesicles containing band 3 protein, the fraction of lipid molecules bound to this protein and the minimum number of sites possessing affinity for phosphatidylinositol-4-phosphate could be approximately estimated. The results of this study indicate that phosphoinositides are located preferentially adjacent to band 3. Intramolecular excimer formation of dipyrene-labeled phosphatidylcholine, phosphatidylinositol, and phosphatidylinositol-4-phosphate yielded information about the acyl chain dynamics of lipids surrounding the protein and of lipids in the bulk membrane. Time-resolved measurements of the pyrene fluorescence anisotropy showed that in membranes of resealed erythrocyte ghost cells the rotational freedom of pyrene-labeled phosphatidylinositol-4,5-bisphosphate is smaller than that of pyrene-labeled phosphatidylcholine. In contrast, no significant differences could be detected when these pyrene lipids were dispersed in dioleoylphosphatidylcholine membranes. It is proposed that the nonrandom distribution of the phosphoinositides induced by lipid−lipid repulsion and protein−lipid attraction will have a profound effect on the phospholipase C-catalyzed hydrolysis of the phosphoinositides into second-messenger molecules.

Phosphatidylinositol-4,5-bisphosphate (PIP_2)[1] and its precursors, phosphatidylinositol-4-phosphate (PIP) and phosphatidylinositol (PI), are intriguing lipids because of their vital importance in the regulation of cellular processes. In addition, their highly negative charge (van Paridon et al., 1986) results in strong lipid−lipid and lipid−protein interaction forces. PI, PIP, and PIP_2 are three major *myo*-inositol-containing lipids, comprising only 2−8% of the total phospholipids present in mammalian cells (Majerus, 1992).

The phosphoinositides are preferentially located on the cytosolic surface of the plasma membrane (Schmell & Lennarz, 1974; Sekar & Hokin, 1986; Gascard et al., 1991). Extensive studies on phosphoinositide metabolism showed that inositide lipids play a key role in the signal transduction cascade (Berridge, 1993; Michell, 1992; Sekar & Hokin, 1986). In response to receptor stimulation or calcium channel opening, the turnover of inositides increases dramatically and phosphodiesteric cleavage of phosphatidylinositols by phospholipase C (PLC) yields the intracellular second messengers diacylglycerol (DG) and various water-soluble inositol phosphates. These messengers trigger a wide range of cellular responses.

In contrast to their role in cellular signalling, relatively little is known about the physical behavior of the phosphoinositides in membranes and their interaction with membrane proteins. Evidence has been obtained that there are distinct pools of phosphoinositides within cells which can be divided on a functional basis into pools that can be hydrolyzed for signal transduction purposes and pools that cannot (King et al., 1987; Koréh & Monaco, 1986; Müller et al., 1986; Cubitt et al., 1990; Monaco & Adelson, 1991; Gascard et al., 1989, 1993a). It has, for example, been observed that only 50−60% of the total phosphoinositides in erythrocyte membranes is accessible for PLC-catalyzed hydrolysis (Gascard et al., 1989). Discrete regions or domains of phosphoinositides that are maintained by integral membrane proteins may form a

† This research was supported by The Netherlands Foundation for Biophysics under the auspices of The Netherlands Organisation for Scientific Research (NWO). A. Hanicak acknowledges with gratitude support by a short-term EMBO fellowship.

* Address correspondence to this author at: Department of Biochemistry, Agricultural University, Dreijenlaan 3, NL-6703 HA Wageningen, The Netherlands.

‡ Agricultural University.

§ J.W. Goethe University.

|| Utrecht University.

⊗ Abstract published in *Advance ACS Abstracts,* June 15, 1995.

[1] Abbreviations: dipyr, *sn*-1,2-bis(pyrenyldecanoyl); DOPC, dioleoylphosphatidylcholine; EDTA, ethylenediaminetetraacetic acid; EGTA, ethylene glycol bis(β-aminoethyl ether)-*N*,*N*,*N*′,*N*′-tetraacetic acid; *EM*, ratio of excimer to monomer fluorescence; MC model, Milling Crowd model; PC, phosphatidylcholine; PI, phosphatidylinositol; PIP, phosphatidylinositol-4-phosphate; PIP_2, phosphatidylinositol-4,5-bisphosphate; PLC, phospholipase C; PS, phosphatidylserine; pyr, *sn*-2-(pyrenyldecanoyl); SSQ, sum of squares of residuals; thesit, poly(oxyethylene-9-lauryl ether); Tris, tris(hydroxymethyl)aminomethane.

0006-2960/95/0434-9118$09.00/0

basis for this metabolic heterogeneity of phosphoinositides (Gascard et al., 1993a), although direct evidence for such domains is difficult to establish.

Besides a second-messenger precursor role, other biological functions for PIP_2 have been discussed. So it has been reported that phosphoinositides interact with membrane proteins like Ca^{2+}-ATPase (Verbist et al., 1991), erythrocyte band 4.1 protein (Gascard et al., 1993b; Hagelberg & Allan, 1990), and band 3 protein (Hanicak et al., 1994) and cytosolic proteins like profilin (Lassing & Lindberg, 1985; Janmey et al., 1987), gelsolin (Janmey & Stossel, 1989; Yin et al., 1988), and protein kinase C (Huang & Huang, 1991; Pap et al., 1993). In addition, these lipids regulate the functioning of Ca^{2+}-ATPase (Missiaen et al., 1989), the EGF receptor (Den Hartigh et al., 1993), and protein kinase C (Huang & Huang, 1991; Pap et al., 1993; O'Brain et al., 1987; Lee & Bell, 1991; Chauhan & Brockerhoff, 1988) and the shape of the erythrocyte (Ferrel & Hyestis, 1984).

The aim of this study is to characterize the physical behavior of phosphoinositides in membranes and their interaction with proteins. To achieve this, phosphoinositides carrying a pyrenedecanoyl moiety as fluorescent reporter group were incorporated in vesicles and biological membranes and the lateral and rotational dynamical characteristics of these probe lipids were determined. The excimer experiments provide information on the intermolecular electrostatic repulsion of the phosphoinositides and the effect of protein on the intermolecular collision frequency. Experiments with dipyrene-labeled analogues of PC, PI, and PIP provide information on the acyl chain dynamics at close proximity of the protein and in bulk lipid. The latter experiments are supported by time-resolved anisotropy experiments of pyrene-labeled PC and PIP_2 in resealed ghost cells and lipid vesicles.

EXPERIMENTAL PROCEDURES

Materials. 1-Palmitoyl-2-(1′-pyrenyldecanoyl)-PC (pyr-PC) was synthesized from egg yolk PC (Sigma) as described by Somerharju and Wirtz (1982). *sn*-2-(1′-Pyrenyldecanoyl)-PI (pyr-PI) was synthesized from yeast PI as described by Somerharju et al. (1985). *sn*-2-(1′-Pyrenyldecanoyl)-PIP (pyr-PIP) and *sn*-2-(1′-pyrenyldecanoyl)-PIP_2 (pyr-PIP_2) were synthesized enzymatically from pyr-PI using partially purified PI and PIP kinase preparations from bovine brain as described by Gadella et al. (1990). *sn*-1,2-Bis(pyrenyldecanoyl)-PC (dipyr-PC) was synthesized by methods described previously (Patel et al., 1979). *sn*-1,2-Bis(pyrenyldecanoyl)-PI (dipyr-PI) and dipyr-PIP were kind gifts of Dr. P. Nieuwenhuizen, University of Utrecht. The experiments were performed using buffer containing 0.5 mM EDTA, 10 mM Tris-HCl, and 50 mM KCl at pH 8.

Methods

Isolation of Band 3 Protein. Band 3 protein was purified as described by Yu and Steck (1975) and Pappert and Schubert (1983) and incorporated into DOPC vesicles by dialysis according to Scheuring et al. (1984).

Incorporation of Pyrene-Labeled Lipids into Membranes. The ghost cell membranes were prepared as described by Wood (1989). Membrane vesicles containing pyrene-labeled lipids were prepared by mixing the fluorescent lipid with the other lipids in ethanol/DMSO (75:25, v/v) and injecting the mixture in buffer under stirring. The protein-enriched vesicles and ghost cell membranes were loaded with pyrene-containing lipids by adding small aliquots (maximum 2% of sample volume) of pyrene lipid stock solutions in ethanol/DMSO (75:25, v/v). The pyrene lipid concentration in the stock solution was measured spectrophotometrically using the extinction coefficient $\epsilon = 39\,700\ M^{-1}\ cm^{-1}$ at 345 nm in ethanol/DMSO. The samples were incubated overnight at 4 °C in an argon-saturated atmosphere prior to fluorescence measurements.

Fluorescence Methods. Pyrene emission intensities were monitored on a DMX-1000 steady state spectrofluorometer (SLM Aminco, Urbana, IL). The measurements were corrected for background emission (sample without pyrene lipid) and spectral instrument characteristics. Excitation and emission bandwidths were set at 4 nm. Monomer and excimer emission was detected at 377 and 487 nm, respectively. The excitation wavelength was set at 347 nm. The sample holder was thermostated at 20 °C.

Fluorescence lifetime and anisotropy decays of samples with probe to lipid molar ratios of 0.005 were measured by use of a time-correlated single-photon counting setup as described elsewhere (Pap et al., 1993). The excitation wavelength was 327 nm, and the fluorescence emission was selected using a WG 360 cutoff filter and an interference filter at 374.6 nm (Schott, Mainz, Germany). After each measurement, the background was measured at one-fifth of the time of sample acquisition. 1,4-Bis[2-(5-phenyloxazolyl)]benzene (Eastman Kodak, Rochester, NY) dissolved in ethanol served as reference compound ($\tau = 1.35$ ns) to yield the dynamical instrumental response function of the setup (Vos et al., 1987). The sample holder was thermostated at 4 °C.

THEORY

Excimer Formation in Lipid Membranes. Pyrene analogues can form excited state dimers (excimers) between one pyrene molecule in the excited state and one in the ground state (Förster & Kasper, 1955). The rate of excimer formation is determined by the collision frequency of pyrene moieties. Therefore, when pyrene analogues are applied in membranes, their excimer formation can report about lateral organization and translational mobility of lipids (Galla & Sackmann, 1974; Eisinger et al., 1986; Vauhkonen et al., 1989, 1990; Sassaroli et al., 1990). For lipids containing one pyrene acyl chain, the process of excimer formation (M + M* → E*) can be described by the following scheme (Vauhkonen et al., 1990):

$$\begin{array}{ccccc} M + M^* & \underset{k_{-1}}{\overset{k_1}{\rightleftharpoons}} & (M,M^*) & \underset{k_{-2}}{\overset{k_2}{\rightleftharpoons}} & E^* \\ \downarrow \tau_m^{-1} & & \downarrow \tau_m^{-1} & & \downarrow \tau_e^{-1} \end{array}$$

in which τ_m^{-1} and τ_e^{-1} (in s^{-1}) represent the fluorescence rate constants of monomer and excimer, respectively. Two dynamic processes govern the excimer formation: first, neighbor formation [M + M* → (M,M*)] which is characterized by the rate constants k_1 and k_{-1}. This process is modeled well with the so-called Milling Crowd (MC) model (Eisinger et al., 1986) which considers lipid probes migrating in a trigonal lattice of lipids by exchanging positions with one of their six nearest neighbors. The rate constant k_1 is related to the frequency of lipids exchanging positions in

the membrane matrix (f) and to the number of lipid exchange events required before (M,M*) is formed (n). Inherent to the trigonal organization of lipids, k_{-1} corresponds approximately to $f/2$ (Sassaroli et al., 1990; Vauhkonen et al., 1990). Second, the reaction leading to formation of E* is governed by the rate constants of association, k_2, and dissociation, k_{-2}, which are related to the rotational freedom and dynamics of pyrene acyl chains. In most kinetic considerations, k_{-2} is assumed much smaller than τ_e^{-1} and therefore negligible. The overall rate of intermolecular excimer formation of monopyrene lipids (k_{ex}) can be expressed by (Eisinger et al., 1986):

$$k_{ex} = \frac{f}{n} \tag{1}$$

where n corresponds to the average number of lipid exchanges required before an excimer is formed. The parameter n is a function of the probe mole fraction (x), of interaction forces between pyrene lipids, and of k_2 (see below, eq 6).

In principle, both k_2 and f can be estimated from least squares fitting of the dependence of the monomeric fluorescence yield (I_m) on the mole fraction of pyrene lipid (Eisinger et al., 1986):

$$\frac{I_m}{I'_m} = \frac{1}{1 + \tau_m k_{ex}} \tag{2}$$

where I'_m corresponds to the monomer intensity obtained at very low mole fraction of pyrene lipid. In practice, however, the quality of the data is such that large errors in the optimized values are obtained resulting in multiple sets of solutions for f and k_2. Therefore it is preferable to determine k_2 in an independent way by using the excimer to monomer fluorescence intensity ratio of lipids containing two pyrene acyl chains (dipyrene lipids) (EM_2) and monopyrene lipids (EM_1) at the critical mole fraction (x_o) (Vauhkonen et al., 1990). At this critical molar probe ratio, the rate of excimer formation is equal to the monomer fluorescence decay rate, τ_m^{-1} (Sassaroli et al., 1990):

$$k_2 = \frac{EM_2}{EM_1(x_o)} \tau_m^{-1} \tag{3}$$

We have adapted the MC model for lipid migration by incorporating a lipid−lipid interaction factor (R). In addition, we have derived a statistical description for n which turns out to be a good alternative for the n values obtained from simulations in previous studies (Eisinger et al., 1986; Sassaroli et al., 1990). It is assumed that pyrene lipids which do not repel each other are randomly distributed (repulsion factor $R = 1$) in the membrane and exchange positions (migrate) with one of their six nearest neighbors. The probability of finding a pyrene lipid at a neighbor position of a certain excited pyrene molecule depends on (1) the pyrene lipid mole fraction in the membrane (x); (2) the interaction forces between the pyrene lipids (when pyrene lipids do repel each other, like in the case of pyr-PIP_2, the randomness of migration is affected and the probability of finding a probe molecule at a position next to a certain excited probe molecule is equal to xR with $R < 1$); (3) the number of neighbors surrounding the excited pyrene (s) [in the MC-model, a trigonal lipid packing is assumed ($s = 6$)]; and (4) the probability of encountering one or more lipids which have been neighbors before (so-called "old" neighbors). In the previous configuration these "old" neighbors did not form an excimer with the excited pyrene. Therefore the probability that the "old" neighbors are pyrene lipids corresponds to xR times the probability that these pyrene neighbors did not form an excimer with the excited pyrene ($1 - P_e$) in the previous configuration. When, for instance, P_e corresponds to unity (pyrene neighbors always lead to excimer formation), the probability that an "old" lipid neighbor is a pyrene is zero. In deriving the probability of finding q pyrene lipids out of s neighbors, we should thus consider all possible combinations of s_o "old" and $s - s_o$ "new" neighbors:

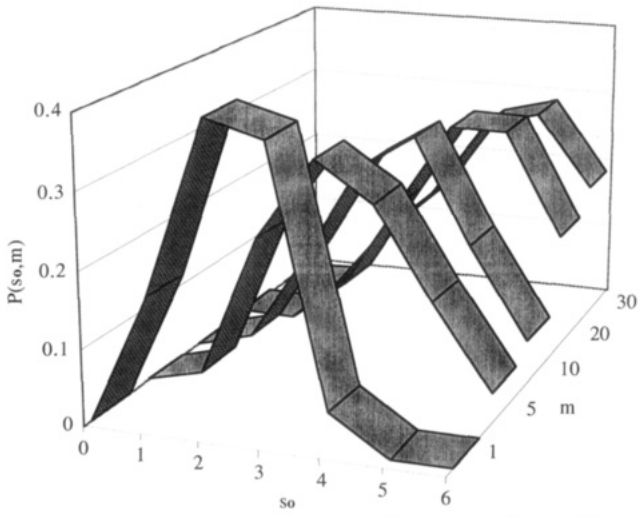

FIGURE 1: Dependence of the probability that s_o "old" neighbors are encountered, on the number of migration steps taken (m).

$$P(s,q,m) = \sum_{s_o=0}^{s} \sum_{q_o=0}^{q_{max}} \varrho(s_o,m) \binom{s_o}{q_o} [xR(1 - P_e)]^{q_o} [1 - xR(1 - P_e)]^{s_o - q_o} \binom{s - s_o}{q - q_o} (xR)^{q - q_o} (1 - xR)^{s - s_o + q_o - q} \tag{4}$$

Where $\varrho(s_o,m)$ corresponds to the probability of finding s_o "old" neighbors after m migration steps. The part $[xR(1 - P_e)]^{q_o}[1 - xR(1 - P_e)]^{s_o - q_o}$ corresponds to the probability that s_o neighbors are previously encountered of which q_o are pyrene and $s_o - q_o$ are not. Likewise, $(xR)^{q - q_o}(1 - xR)^{s - s_o - q + q_o}$ corresponds to the probability that $s - s_o$ neighbors are newly encountered of which $q - q_o$ are pyrene lipids and $s - s_o - q + q_o$ are not. The two binomial terms correspond to the number of ways how q_o molecules can be rearranged at s_o positions or $q - q_o$ molecules at $s - s_o$ positions. The summation is carried over $s_o = 0$ to s and $q_o = 0$ to either $q_{max} = q$ or, if s_o is smaller than q, $q_{max} = s_o$. The probability function $\varrho(s_o,m)$ was obtained from simulations of lipids migrating in a trigonal lipid matrix by exchanging positions with one of their randomly chosen neighbors. After each step, the number of neighbors that already encountered the excited pyrene in one of the previous configurations is stored. The results of these simulations are given in Figure 1. It is obvious from this figure that the probability of encountering "old" neighbors increases with

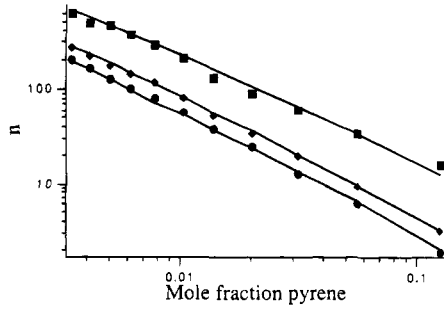

FIGURE 2: Dependence of the average number of lipid exchange events of an excited pyrene before an excimer is formed (n) on the mole fraction of pyrene probe (x) in membranes. No repulsive or attractive interaction forces were taken into account ($R = 1$). The points were obtained from random walk simulations of an excited pyrene lipid in a trigonal lipid matrix with periodic boundaries containing various mole fractions of nonexcited pyrene lipids. Both excited and nonexcited pyrenes migrated by exchanging positions with one of their randomly chosen six neighboring lipids. After each relocation of the pyrene lipids, the program tested if an excimer was formed for $P_e = 0.1$ (■), 0.5 (◆), and 1 (●). All lipids were randomly repositioned when an excimer was formed. The points correspond to the total number of steps taken divided by the number of excimers formed. The curves through the points were obtained for the corresponding P_e values with the statistical description of n as described in eq 6. See the theoretical section for further details.

m. From the kinetic scheme it can be derived that the probability that two pyrene neighbors form an excimer (P_e) is equal to $k_2/(k_2 + f/2 + \tau_m^{-1})$. Then the probability that a pyrene lipid surrounded by q neighboring pyrene lipids will not form an excimer corresponds to $(1 - P_e)^q$. These considerations lead to the following equation for the probability that the excited pyrene survives the mth step:

$$P^s(f,k_2,m) = \sum_{q=0}^{s} P(s,q,m)(1 - P_e)^q \qquad (5)$$

The probability that an excimer is formed in the mth step is a product of the probability that it is not formed in the previous steps (the product term between brackets in eq 6) and the probability that it is formed in the mth step $[1 - P^s(f,k_2,m)]$. We can then write for n:

$$n = \sum_{m=1}^{\infty} m[[\prod P^s(f,k_2,i)](1 - P^s(f,k_2,m))] \qquad (6)$$

In order to prove the validity of eq 6, random walk simulations were performed similar to those described earlier (Eisinger et al., 1986; Sassaroli et al., 1990). Figure 2 shows that the values for n obtained from these simulations (points) and from eq 6 (lines) show that the model fits random walk simulations with high precision for various values of P_e.

Two-Domain Model for Excimer Formation in the Presence of Band 3 Protein. The coexistence of proteins in the plane of the biological membrane has several important consequences for in-plane lipid diffusion. Proteins act as simple physicochemical barriers of lipids. The effect of proteins on the long-range diffusion of lipids has been evaluated by Eisinger et al. (1986). These authors performed simulations with the MC model in which proteins were considered as lipid-forbidden hexagons in the bilayer. In addition, three effects contribute to a protein-induced reduction of the excimer formation of pyrene lipids. (1) Proteins statistically reduce the excimer formation by occupying neighboring positions of probe lipids and thus affecting the parameter s of eq 5. (2) Lipids interacting at the protein surface are laterally immobilized and exchange positions with neighboring lipids only slowly. The exchange frequency of bound lipids (f_b) might be significantly lower than that of lipids in the bulk lipid matrix (f_f). (3) Flexible lipid chains adjacent to proteins will adapt to the protein surface. This accommodation will affect the rotational dynamics and angular freedom of the lipid probes. Therefore a k_{2b} for protein-bound pyrene lipids has to be defined apart from a k_{2f} for noninteracting pyrene lipids.

In order to include these effects in the description for excimer formation, we have to derive the fraction of pyrene lipids adjacent to a protein. We assume that a protein is surrounded by j lipid positions (B) which are occupied either by a pyrene lipid (P) or a nonlabeled lipid (L). The relative binding constant (K) of a certain lipid positioned adjacent to the protein is equal to the ratio of the association constants for P and L occupying this position:

$$L + BP \rightleftarrows P + BL;\ K = \frac{K_P}{K_L} = \frac{[L][BP]}{[P][BL]} \qquad (7)$$

The average fractional occupancy (γ) of a protein lipid site with pyrene lipid is a function of the relative concentration of the individual components in this equilibrium:

$$\gamma = \frac{[BP]}{[BP] + [BL]} \qquad (8)$$

Since K is a relative constant, it is independent of the actual concentration of pyrene lipid and protein. Only the protein to lipid molar ratio (ϱ) and pyrene mole fraction (x) are relevant parameters. If $K = 1$ (equal interaction forces between the protein surface and the pyrene lipid and unlabeled lipid), the fractional occupancy of a lipid position adjacent to the protein will be equal to x. In case of $K \neq 1$, one can derive an expression for the fractional occupancy from mass balance relationships and eqs 7 and 8:

$$\gamma = \frac{1}{2(K-1)j\varrho}[1 - j\varrho + Kj\varrho - x(1-K) - \sqrt{-4(-1+K)Kj\varrho x + (-1 + j\varrho - Kj\varrho + x - Kx)^2}] \qquad (9)$$

From the average number of pyrene lipids per protein or "protein occupancy", $\langle J \rangle$ ($=\gamma/j$), the fraction of pyrene lipids (ν) located next to a protein can be calculated

$$\nu = \frac{\langle J \rangle \varrho}{x} \qquad (10)$$

Protein hexagons in a trigonal (lipid) matrix have six lipid positions with five lipid neighbors and $j - 6$ positions with four lipid neighbors. If we neglect the probability that a pyrene lipid molecule is interacting with more than one protein, the following expression for the probability of excimer formation is obtained after m steps in protein-containing membranes:

$$P(f,k_2,m) = 1 - \left[\frac{\nu(j-6)}{j} P^{s=4}(f_b,k_{2b},m) + \frac{\nu 6}{j} P^{s=5}(f_b,k_{2b},m) + (1-\nu)P^{s=6}(f_f,k_{2f},m)\right]^m \qquad (11)$$

Table 1: Ratio of Excimer to Monomer Fluorescence of Dipyrene-Labeled Analogues of PC, PI, and PIP in DOPC Vesicles, DOPC Vesicles Containing Band 3 Protein, and Resealed Ghost Cell Membranes[a]

probe/lipid system	EM_2	$EM_1(x_o)$	k_2 ($\times 10^7$ s^{-1})
dipyr-PC/DOPC	0.226 (0.03)	0.15	1.13
dipyr-PI/DOPC	0.221 (0.04)		1.09
dipyr-PIP/DOPC	0.245 (0.04)		1.20
dipyr-PC/band 3	0.248 (0.04)	0.16	1.17
dipyr-PI/band 3	0.225 (0.05)		1.05
dipyr-PIP/band 3	0.204 (0.05)		0.98
dipyr-PC/ghost	0.241 (0.03)	0.18	0.98
dipyr-PI/ghost	0.201 (0.04)		0.83
dipyr-PIP/ghost	0.157 (0.02)		0.64

[a] The values in parentheses correspond to standard errors of average values obtained from three experiments. The EM_1 value determined for pyr-PC was used in the calculation of k_2 of all dipyrene-labeled lipids according to eq 3. This approach is validated by the fact that the EM_1 value at the critical mole fraction is not dependent on dynamic properties. The protein−lipid molar ratio was 1:140 for ghost cell membranes and 1:1000 for the band 3 protein reconstitutions. The experiments were performed at 20 °C.

This equation can be applied to eq 6 yielding an extended expression for n in protein-containing membranes. For the calculation of k_{ex} (eq 1), f is divided similarly into fraction ν of protein-bound lipids with exchange frequency f_b and fraction $1 - \nu$ of lipids in the bulk membrane with exchange frequency f_f.

RESULTS

Model-Independent Determination of k_2. In order to estimate the rate constant of excimer formation of two neighboring pyrene moieties (k_2), we performed an experiment with dipyr-PC, dipyr-PI, and dipyr-PIP in DOPC vesicles, DOPC vesicles containing band 3 protein, and resealed ghost membranes. In each experiment the lipid to probe molar ratio was smaller than 0.005, so that intermolecular excimer formation can be neglected (Somerharju et al., 1985). The ratios of excimer to monomer fluorescence (EM_2) of dipyr-PC, dipyr-PI, and dipyr-PIP in these membrane systems are listed in Table 1. As described in the theoretical section, k_2 is related to the EM value of dipyrene lipids, the EM_1 value of monopyrene lipids at the critical mole fraction, and the average monomer fluorescence lifetime. The value of the monomer fluorescence lifetime (τ_m = 133 ns) used in this calculation was obtained independently from fluorescence decay measurements. In this lifetime determination, only the predominant long-lived component has been considered, which is in agreement with measurements of van den Zegel et al. (1984) and Sassaroli et al. (1990).

The calculated k_2 values show some interesting features (Table 1). For dipyr-PC, only a 10% reduction of k_2 is observed when the pyrene lipids are dispersed in ghost cell membranes. This indicates that the "microfluidity" experienced by this probe differs only slightly in the different membrane systems. In DOPC membranes, the k_2 values of the three different dipyrene lipids are approximately equal. The differences in headgroup moieties apparently do not influence the collision frequency of the pyrenes at both acyl chains. A considerable reduction of the k_2 value of especially dipyr-PIP is observed when dispersed in protein-containing membranes. This reduction of k_2 is particularly large in the resealed ghost cell membranes, having relatively high protein content. This implies that phosphoinositides interact to a higher extent with the membrane proteins than dipyr-PC and as a consequence experience a more rigid environment.

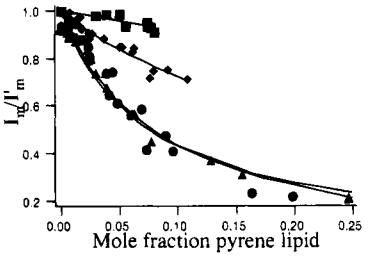

FIGURE 3: Dependence of the normalized monomeric fluorescence intensity on the mole fraction of incorporated pyrene-labeled PC (●), PI (▲), PIP (◆), and PIP_2 (■) in DOPC vesicles. The curves are the best fits obtained by applying eqs 2 and 6 to the experimental points, giving results listed in Table 2. The experiments were performed at 20 °C.

Monomer Fluorescence in DOPC Vesicles. The normalized monomer fluorescence emission obtained after titration of various monopyrene lipids in DOPC membranes is given in Figure 3. The negatively charged pyr-PI and the electrically neutral pyr-PC have a similar dependence of the monomer quenching on their mole fraction. The collision frequency of the higher phosphorylated inositide lipids pyr-PIP and pyr-PIP_2, however, is substantially lower at comparable mole fractions in membranes. The relatively bulky headgroup of inositide lipids may contribute to a lower lateral diffusion coefficient. We assume, however, that diffusion of pyrene lipids is mainly dependent on the host lipid matrix, and thus the effect of the various probe lipid headgroups on the lipid exchange frequency (f) can be neglected. This approximation holds true only at low mole fractions of pyrene lipid in the membranes. Repulsive electrostatic interactions between the phosphorylated headgroups of the inositides will lower the probability that two pyrene-labeled inositide lipids become each other's nearest neighbor (and thus there will be an effect on n). The repulsion factor (R) between the two pyrene-labeled inositide lipids can be estimated by applying the extended MC model to the normalized monomeric yields of the various lipids (see the theoretical section). In this approach we assume that pyr-PC's in a DOPC environment do not repel or attract each other (R = 1). Analysis of the monomeric pyr-PC fluorescence with the extended MC model using the value for k_2 obtained from the former dipyrene experiments yielded optimal fits with a value for f of 3.14 10^7 s^{-1}. Application of k_2 and f in analyses of the monomeric data of pyr-PI, pyr-PIP, and pyr-PIP_2 (Figure 3) yielded R values of 1, 0.34, and 0.14, respectively (Table 2). We can thus conclude that a PIP_2 lipid prefers more than 7 times a neutral lipid neighbor than another PIP_2 molecule as a neighbor. Therefore, the polyvalent phosphoinositides will be nonrandomly distributed in the membrane.

Monomer Fluorescence in DOPC Vesicles Containing Band 3. The dependence of the monomer fluorescence on the mole fraction of monopyrene inositide lipids in band 3 protein reconstituted in DOPC vesicles is given in Figure 4. From comparison with Figure 3, two major conclusions can be drawn. (1) Band 3 protein reduces the number of intermolecular collisions of the pyrene inositide. (2) The affinity of band 3 protein for inositides is limited. Multiple sites with high affinity for the pyrene lipids should lead to

Table 2: Values of Dynamical (f, D) and Repulsive (R) Parameters Recovered from the Analysis of the Normalized Monomer Fluorescence Yield of the Various Pyrene-Labeled Lipids[a]

probe	f ($\times 10^7$ s^{-1})	D (μm^2 s^{-1})	R	SSQ[b]	charge
pyr-PC	3.14 (2.89, 4.34)	5.5	1	0.0013	0
pyr-PI	1	5.5	1 (0.86−1.27)	0.0034	−1
pyr-PIP	1	5.5	0.34 (0.30−0.37)	0.0005	−2.9
pyr-PIP$_2$	1	5.5	0.14 (0.09−0.18)	0.0003	−4.2

[a] In the analysis, k_2 was fixed to 1.13×10^7 s^{-1} (Table 1). The lateral diffusion coefficient was calculated according to $f\lambda^2/4$ (Eisinger et al., 1986), where λ corresponds to the lipid−lipid spacing ($\lambda^2 = 70$ nm^2 for DOPC; Demel et al., 1967). The values in parentheses correspond to the errors at a 67% confidence level as determined from the dependence of the SSQ on the value of the examined parameter [see Beechem et al. (1991)]. The net charge of the lipids at pH 7.4 is given in the last column (van Paridon et al., 1986). [b] $SSQ = 1/N\sum_{i=1}^{N}(\text{data}_i - \text{fit}_i)^2$ for N data points.

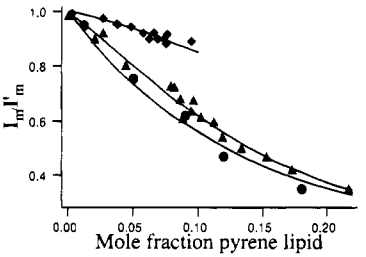

FIGURE 4: Dependence of the normalized monomeric fluorescence intensity on the mole fraction of incorporated pyrene-labeled PC (●), PI (▲), and PIP (◆) in band 3 protein reconstituted in DOPC vesicles. The curves are the best fits obtained by applying the two-domain model to the experimental points (see the theoretical section). The experiments were performed at 20 °C.

a sigmoidal dependence of the monomer intensity on the concentration of pyrene lipids added. In other words, even at higher mole fractions of pyrene lipids, there are (lipid) positions next to the protein that are not occupied by a pyrene lipid. As described in the theoretical section, protein-induced reduction of excimer formation originates from statistical factors and from differences in local order and dynamics of lipids in the vicinity of proteins. The complex relationship for excimer formation in protein-rich membranes is embodied in the model in which many parameters have to be determined. This number can, however, be drastically reduced if the optimized values of the independent analysis of lipids in DOPC are used to obtain both R and f_f. This step is validated by the fact that DOPC was used as a host lipid in both the reconstitution of band 3 protein and the titration experiments described in Figure 3. We thus neglect effects of proteins on the lipid−lipid (electrostatic) interaction forces (R). Since the excimer formation of dipyr-PC is hardly affected by the presence of protein (Table 1), its k_2 value is representative for lipids that do not interact with protein (k_{2f}). On the other hand, the excimer formation of dipyr-PIP is significantly influenced by proteins. The value of the rate constant k_2 will thus represent a mean value composed of dipyr-PIP molecules interacting with band 3 protein and dipyr-PIP molecules residing in bulk lipid. Therefore, k_2 of dipyr-PIP can be considered as an upper limit for k_2 of lipids that interact with the protein (k_{2b}). The protein−lipid ratio (PL) is determined chemically (PL = 0.001; see the Methods section), and the size of band 3 protein in membranes is approximately 66 Å in diameter as

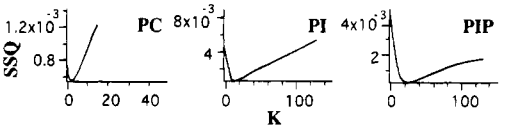

FIGURE 5: SSQ search of the average relative binding constant (K) of band 3 for pyr-PC, pyr-PI, and pyr-PIP as obtained by applying the two-domain model (see the Methods section) to the data of Figure 4. In the analysis, the parameters f_b and k_b were fixed to 0 and 6.4×10^6 s^{-1}, respectively.

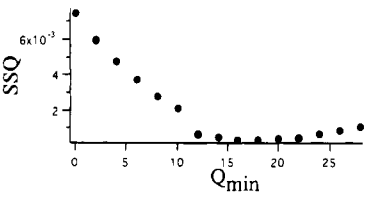

FIGURE 6: SSQ plot of the analysis of the pyr-PIP data in Figure 4 as a function of the number of high-affinity sites (Q). In this two-domain analysis, it is assumed that S sites possess high affinity for pyr-PIP (K was set to 10^9), while the others ($j - Q$) do not (K = 1). In order to obtain an absolute minimum, the parameters f_b and k_b were both fixed to 0 s^{-1}.

was determined from electron microscopic analysis of band 3 crystals (Wang et al., 1993; Dolder et al., 1993). This corresponds to approximately 72 lipids surrounding the protein. When we assume that the fluorescence lifetime is short relative to the mean residence time of a pyrene lipid at the protein surface ($f_b = 0$), the two-domain model can now be applied to the excimeric data given in Figure 4 with only K as the constrained adjustable parameter ($K \geq 1$). The SSQ searches of these analyses are presented in Figure 5. As can be expected for a labeled PC lipid in PC membranes, the average affinity of pyr-PC for band 3 relative to the bulk DOPC is negligible. The SSQ minimum is well defined to a K value of 2, which is, in view of the inexact estimates of several parameters in this analysis and the simplicity of the two-domain model, a satisfying result. For pyr-PI and pyr-PIP, the optimal K values amounted to 14 and 22, respectively. These K values are rough indices of the average relative affinity of the pyrene lipids for the band 3 surface. On the basis of this analysis, one may conclude that the average time that a pyr-PIP molecule is located near the band 3 surface is approximately 20 times longer than that of a DOPC molecule. If one assumes that only a selective number (Q) of the total lipid sites (j) on the band 3 protein possesses high affinity for pyr-PIP ($K \rightarrow \infty$), while the remaining surface ($j - Q$) has no affinity for pyr-PIP (K = 1), and one assumes that the interacting pyr-PIP lipids do not form excimers ($k_b, f_b = 0$), a minimal number of affinity sites for pyr-PIP can be estimated (Q_{min}) (see Figure 6).

Rotational Dynamics of Pyrene-Labeled Lipids in Ghost Cell Membranes. Next to the lateral organization and dynamics, pyrene probes offer also the possibility to study rotational dynamics by means of fluorescence anisotropy decay. The influence of protein−lipid interactions on the rotational dynamics of the pyrene-labeled lipids was characterized further by measuring the polarized fluorescence decays of the lipid probes in resealed ghost cells and DOPC membranes. From these decays the anisotropy was constructed, which is presented for PIP$_2$ and PC in Figure 7. For this technique, however, the properties of pyrene are not so suitable since the fluorescence lifetime is 1 order of magnitude longer than the reorientational dynamics of the

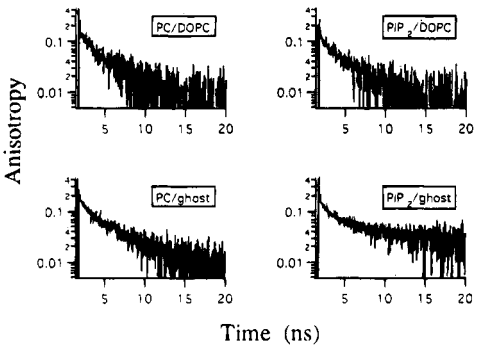

FIGURE 7: Experimental fluorescence anisotropy decays of pyr-PC and pyr-PIP_2 in DOPC and erythrocyte ghost cell membranes. The experiment was performed at 4 °C.

probe in vesicles (which considerably prolongs the experiment), and in addition, the theoretical treatment of the rotational motion is extremely complex (Zannoni et al., 1983). Therefore detailed interpretation is omitted, and the results are qualitatively described. Some interesting features are nonetheless obtained from these experiments. In DOPC membranes, the fluorescence anisotropy of both pyr-PIP_2 and pyr-PC declines to zero at longer times. This indicates that the rotation of the pyrene chains in these membranes is not restricted on the time scale of the relatively long lifetime. However, in the protein-rich ghost cells, the fluorescence anisotropy of pyr-PIP_2 has a finite value at longer times, indicating that its motion is restricted. In contrast, the pyr-PC analogue is able to rotate free in the membrane. The acyl chain moieties of PIP_2 are apparently interacting with the protein surface and therefore are constrained in their motions.

DISCUSSION

In this study we have characterized the effect of repulsive electrostatic lipid−lipid forces on the randomness of the distribution of pyrene-labeled phosphoinositides in membranes. In addition, the effect of interaction with band 3 protein on the lateral organization and dynamic properties of these labeled lipids was evaluated. Registration of excimer formation of pyrene analogues appeared to be very suitable for quantitative analysis of interactions between particular lipid species and between lipids and proteins. From our experiments we conclude that the spatial distribution of polyphosphoinositides in membranes is organized to some extent. Values of 0.09 and 0.33 were obtained for the lipid−lipid repulsion factor R of PIP_2 and PIP. Differences in the lateral organization of PI and PC in DOPC membranes were not observed. Since R is defined as the probability ratio to find a pyrene lipid or a nonlabeled lipid at a certain position next to a pyrene lipid when present at equal mole fractions, this implies that PIP_2 prefers 7 times more a electrically neutral PC neighbor than one of its own species. For the less phosphorylated inositides, PIP and PI, this preference is 3 and 1, respectively. This observation thus excludes the possibility of segregated domains of pure phosphoinositides which are PLC accessible or resistant. Such pools with special properties and compositions have been suggested repeatedly in the literature for other (acidic) lipids (Karnovsky et al., 1982; Levin et al., 1985; Wolf et al., 1988).

The excimer experiments in DOPC containing band 3 protein and in ghost cells indicate that phosphoinositides are located preferentially adjacent to band 3. The phosphoryl moieties of the phosphoinositides probably interact electrostatically with positively charged amino acid residues at the protein surface. This observation does not necessarily imply that band 3 is regulated by the phosphoinositides. Analysis with the two-domain model yielded that there are at least 15 sites with affinity for PIP. Therefore, a specific allosteric function of phosphoinositides is not likely, but the relevance of the interactions for the biological function of band 3 has to be systematically investigated further. From a catalytic point of view of certain enzymes like phospholipase C, the results may have some bearing. The ghost cell membranes used in our experiments consisted of only 140 lipid molecules/integral protein molecule, which is typical for natural membranes (Newton, 1993). Considering this high protein to lipid ratio, the relative binding constant of polyphosphoinositides for abundant proteins like band 3 protein, and the large differences in protein and lipid molecular surfaces, the majority of the phosphoinositides will be in direct contact with protein surfaces. The nonrandom distribution of the phosphoinositides and their interactions with membrane proteins like band 3 might reduce the accessibility of the phosphoinositides for PLC and even be rate limiting for the second-messenger production.

Interactions with membrane proteins could play a role in the mechanism that differentiates accessible from inaccessible phosphoinositides. PLC-inaccessible phosphoinositides could strongly interact with shielded protein segments that prevent interaction with PLC. Phosphoinositides of the accessible pools could diffuse freely in the membrane or could interact with exposed membrane proteins (Gascard et al., 1993a). This speculation agrees well to several observations of other research groups: (1) About 70% of the PIP and 20% of the PIP_2 molecules turn over rapidly (Gascard et al., 1989). This difference can be ascribed to a larger fraction of PIP_2 interacting with protein surfaces. (2) The majority of the PLC-sensitive phosphoinositides appears to be newly synthesized and not already present in the membrane. Lassing and Lindberg (1990) observed that stimulation of kinases phosphorylating PI and PIP precedes the activation of receptor-linked PLC. In addition, Gascard and co-workers (1989) observed that newly synthesized molecules of PIP_2 in erythrocyte membranes are initially accessible to PLC but are subsequently transferred toward a PLC-resistant pool. In addition, recent evidence has been obtained that the PI-transfer protein is required for prolonged PLC activity in permeabilized HL60 cells (Thomas et al., 1993). The authors proposed that the PI-transfer protein is involved in transporting PI from intracellular compartments for conversion to PIP_2 prior to hydrolysis by PLC. A different view is given by Gascard and co-workers, who proposed, on the basis of phospholipase A_2 assay, that PLC-catalyzed hydrolysis of PIP_2 and PIP is facilitated through their interactions with proteins (Gascard et al., 1993). It is, however, hard to visualize how proteins may enhance the accessibility of the phosphoinositides for PLC.

ACKNOWLEDGMENT

We have benefited greatly from the comments of one anonymous referee.

REFERENCES

Beechem, J. M., Gratton, E., Ameloot, M., Knutson, J. R., & Brand, L. (1991) in *Topics in Fluorescence Spectroscopy* (Lakowicz, J. R., Ed.) Vol. 2, Plenum Press, New York.

Berridge, M. J. (1993) *Nature 361*, 315−325.

Chauhan, V. P. S., & Brockerhoff, H. (1988) *Biochem. Biophys. Res. Commun. 155*, 18−23.

Cubitt, A., Zhang, B., & Gershengorn, C. (1990) *J. Biol. Chem. 265*, 9707−9714.

Demel, R. A., Van Deenen, L. L. M., & Pethica, B. A. (1967) *Biochim. Biophys. Acta 135*, 11−19.

Den Hartigh, J. C., van Bergen Henegouwen, P. M. P., Boonstra, J., & Verkleij, A. J. (1993) *Biochim. Biophys. Acta 1148*, 249−262.

Dolder, M., Walz, T., Hefti, A., & Engel, A. (1993) *J. Mol. Biol. 231*, 119−132.

Eisinger, J., Flores, J., & Petersen, W. P. (1986) *Biophys. J. 49*, 987−1001.

Ferrel, J. E., & Huestis, W. H. (1984) *J. Cell. Biol. 98*, 1992−1998.

Förster, Th., & Kasper, K. (1955) *Z. Elektrochem. 59*, 976−980.

Gadella, T. W. J., Moritz, A., Westerman, J., & Wirtz, K. W. A. (1990) *Biochemistry 29*, 3389−3395.

Galla, H. J., & Sackman, E. (1974) *Biochim. Biophys. Acta 339*, 103−115.

Gascard, P., Journet, E., Sulpice, J. C., & Giraud, F. (1989) *Biochem. J. 264*, 547−553.

Gascard, P., Tran, D., Sauvage, M., Sulpice, J. C., Fukami, K., Takenawa, T., Claret, M., & Giraud, F. (1991) *Biochim. Biophys. Acta 1069*, 27−36.

Gascard, P., Sauvage, M., Sulpice, J. C., & Giraud, F. (1993a) *Biochemistry 32*, 5941−5948.

Gascard, P., Pawelczyk, T., Lowenstein, J. M., & Cohen, C. M. (1993b) *Eur. J. Biochem. 211*, 671−681.

Hagelberg, C., & Allan, D. (1990) *Biochem. J. 271*, 831−834.

Hanicak, A., Maretzki, D., Reimann, B., Pap, E. H. W., Visser, A. J. W. G., Wirtz, K. W. A., & Schubert, D. (1994) *FEBS Lett. 348*, 169−172.

Huang, F. L., & Huang, K. P. (1991) *J. Biol. Chem. 266*, 8727−8733.

Janmey, P. A., & Stossel, T. P. (1989) *J. Biol. Chem. 264*, 4825−4831.

Janmey, P. A., Iida, K., Yin, H. L., & Stossel, T. P. (1987) *J. Biol. Chem. 262*, 12228−12236.

Karnovsky, M. J., Kleinfeld, A. M., Hoover, R. L., & Klausner, R. D. (1982) *J. Cell. Biol. 94*, 1−6.

King, C. E., Stephens, L. R., Hawkins, P. T., Guy, G. R., & Michell, R. H. (1987) *Biochem. J. 244*, 209−217.

Koréh, K., & Monaco, M. E. (1986) *J. Biol. Chem. 261*, 88−91.

Lassing, I., & Lindberg, U. (1985) *Nature 314*, 472−474.

Lassing, I., & Lindberg, U. (1990) *FEBS Lett. 262*, 231−233.

Lee, M. H., & Bell, R. M. (1991) *Biochemistry 30*, 1041−1049.

Levin, I. W., Thompson, T. E., Barenholz, Y., & Porter, N. A. (1985) *Biochemistry 24*, 6282−6286.

Majerus, P. W. (1992) *Annu. Rev. Biochem. 61*, 225−250.

Michell, R. H. (1992) *Trends Biochem. Sci. 17*, 274−276.

Missiaen, L., Raeymaekers, L., Wuytack, F., Vrolix, M., De Smedt, H., & Casteels, R. (1989) *Biochem. J. 263*, 687−694.

Monaco, M. E., & Adelson, J. R. (1991) *Biochem. J. 279*, 337−341.

Muller, E., Hegewald, H., Jaroszewicz, K., Cumme, G. A., Hoppe, H., & Frunder, H. (1986) *Biochem. J. 235*, 775−783.

Newton, A. C. (1993) *Annu. Rev. Biophys. Biomol. Struct. 22*, 1−25.

O'Brain, C. A., Arthur, W. L., & Weinstein, I. B. (1987) *FEBS Lett. 214*, 339−342.

Pap, E. H. W., Bastiaens, P. I. H., Borst, J. W., van den Berg, P. A. W., van Hoek, A., Snoek, G. T., Wirtz, K. W. A., & Visser, A. J. W. G. (1993) *Biochemistry 32*, 13310−13317.

Pappert, G., & Schubert, D. (1983) *Biochim. Biophys. Acta 730*, 32−40.

Patel, K. M., Morrisett, J. D., & Sparrow, J. T. (1979) *J. Lipid Res. 20*, 674−677.

Ruocco, M. J., & Shipley, G. G. (1982) *Biochim. Biophys. Acta 691*, 309−320.

Sassaroli, M., Vauhkonen, M., Perry, D., & Eisinger, J. (1990) *Biophys. J. 57*, 281−290.

Scheuring, U., Kollewe, K., & Schubert, D. (1984) *Hoppe-Seyler's Z. Physiol. Chem. 365*, 1056−1057.

Schmell, E., & Lennarz, W. J. (1974) *Biochemistry 13*, 4114−4121.

Sekar, M. C., & Hokin, L. E. (1986) *J. Membr. Biol. 89*, 193−210.

Somerharju, P. J., & Wirtz, K. W. A. (1982) *Chem. Phys. Lipids 30*, 81−91.

Somerharju, P. J., Virtanen, J. A., Eklund, K. K., Viano, P., & Kinnunen, P. K. J. (1985) *Biochemistry 24*, 2773−2781.

Thomas, G. M. H., Cunningham, E., Fensome, A., Ball, A., Totty, N. F., Truong, O., Justing Hsuan, J., & Cockcroft, S. (1993) *Cell 74*, 919−928.

van Paridon, P. A., de Kruijff, B., Ouwekerk, R., & Wirtz, K. W. A. (1986) *Biochim. Biophys. Acta 877*, 216−219.

van den Zegel, S., Boens, N., & de Schrijver, F. C. (1984) *Biophys. Chem. 20*, 333−345.

Vauhkonen, M., Sassaroli, M., Somerharju, P., & Eisinger, J. (1989) *Eur. J. Biochem. 186*, 465−471.

Vauhkonen, M., Sassaroli, M., Somerharju, P., & Eisinger, J. (1990) *Biophys. J. 57*, 291−300.

Verbist, J., Gadella, T. W. J., Raeymaekers, L., Wuytack, F., Wirtz, K. W. A., & Casteels, R. (1991) *Biochim. Biophys. Acta 1063*, 1−6.

Vos, K., van Hoek, A., & Visser, A. J. W. G. (1987) *Eur. J. Biochem. 165*, 55−63.

Wang, D. N., Kuhlbrandt, W., Sarabia, V. E., & Reithmeier, R. A. F. *EMBO J. 12*, 2233−2239.

White, D. A. (1973) in *Form and function of phospholipids* (Ansell, G. B., Dawson, R. M. C., & Hawthorne, J. M., Eds.) pp 445−482, Elsevier, Amsterdam.

Wolf, D. E., Libscomb, A. C., & Maynard, V. M. (1988) *Biochemistry 27*, 860−865.

Wood, P. G. (1989) *Methods Enzymol. 173*, 346−355.

Yin, H. L., Iida, K., & Janmey, P. A. (1988) *J. Cell Biol. 106*, 805−812.

Yu, J., & Steck, T. L. (1975) *J. Biol. Chem. 250*, 9176−9184.

Zannoni, C., Arcioni, A., & Cavatorta, P. (1983) *Chem. Phys. Lipids 32*, 179−250.

BI941734P